Article

Journal of Vibration and Control
2020, Vol. 0(0) 1–13

DOI: 10.1177/1077546320938183
journals.sagepub.com/home/jvc
SAGE

Robust integral sliding mode control of tower cranes

Lobna T Aboserre[1] and Ayman A El-Badawy[1,2]

Abstract

In this study, integral sliding mode control is proposed for tower cranes to ensure precise tracking of the desired position while reducing the oscillations of the payload. The nonlinear robust controller is designed based on high fidelity nonlinear dynamical model, unlike the decoupled or linearized models used in the literature. The advantage of this approach is reducing the model uncertainties resulting in a lower control effort demand that would be required by the sliding mode controller. Moreover, the stability of the under-actuated tower crane system is analyzed using Lyapunov theory to guarantee the practical stability of error dynamics. Experimental results of the proposed control approach are compared with conventional sliding mode control to show its effectiveness and robustness against real system uncertainties.

Keywords

Tower crane, under-actuated system, coupled dynamics, integral sliding mode control

1. Introduction

Cranes have been the subject of research for decades because of their importance in many fields and can be classified into several types; tower cranes, rotary cranes, and overhead cranes. Tower cranes are the main focus of this study for their important role in transporting heavy loads during construction. The transportation process of the payload is required to have high speed, minimum swing, and precision of destination, to raise its efficiency and productivity.

Tower cranes are considered as strong mechanical systems which exhibit complicated nonlinear dynamics. Also, they are under-actuated systems with only two inputs to control four degrees of freedom (DOF). The unactuated DOF are the oscillations of the payloads that are required to be eliminated by the controller. Therefore, the complexity of designing a controller is increased compared with fully actuated systems.

Many researchers have developed different controllers for overhead cranes to handle uncertainties that arise in practical implementations, including adaptive control proposed by Yang and Yang (2007), Cho and Lee (2008), and Le et al. (2012), fuzzy controller by Antic et al. (2012) and Aksjonov et al. (2015). Also, robust sliding mode control (SMC) has been proposed by Vázquez et al. (2015) and Qian and Yi (2016).

In the review of Abdel-Rahman et al. (2003), the proposed controllers for tower cranes are fewer than overhead cranes because of its complexity. The main aim of tower cranes' controllers is to eliminate the oscillations of the payload that arise during the transportation process and more specifically in fast maneuvers.

Parker et al. (1995) proposed an open-loop optimal control technique using a simplified model for the tower crane. The optimization problem was solved using dynamic programming and the results showed effectiveness in reducing the oscillations but ignored the effect of parameter variations. Golafshani and Aplevich (1995) generated optimal cargo trajectory tracking solutions using an iterative algorithm. In the meanwhile, the oscillation of the payload was significant even at steady state. Besides optimal control, Al-Mousa (2000) proposed a fuzzy logic and time-delayed position feedback controllers.

Most of the previous work is based on the assumption of a friction-less system. In the real system, friction has a strong impact on the dynamics of the tower crane and should be included in the controller design. Therefore, Omar and Nayfeh (2005) used the gain-scheduling control

[1]Mechatronics Engineering Department, German University in Cairo, Egypt
[2]Mechanical Engineering Department, Al-Azhar University, Egypt

Received: 23 July 2019; accepted: 25 May 2020

Corresponding author:
Ayman A El-Badawy, Faculty of Engineering and Materials Science, German University in Cairo - GUC, New Cairo City - Main Entance, Al Tagamoa Al Khames, Cairo 11835, Egypt.
Email: ayman.elbadawy@guc.edu.eg

law and a laboratory tower crane by considering the friction factor to enhance the study (Al-Mousa, 2000). The controller gains were scheduled to facilitate the suppression of payload vibration within one cycle at the trolley destination.

Another approach to controlling the tower crane system is by using feedforward control techniques. The input shaping method was used by Vaughan et al. (2010) and Samin et al. (2013) to reduce the system's sways at response modes. The control input is developed through consideration of the physical and swaying properties of the system. However, these approaches often lack robustness concerning parametric uncertainties (such as varying mass and friction coefficients), external disturbances and could not damp residual swing well.

Various techniques based on closed-loop systems which are known to be less sensitive to parametric uncertainties and external disturbances were proposed such as the robust adaptive control by He et al. (2014) and iterative learning control by He et al. (2018). Elbadawy and Shehata (2015) and Ahmad et al. (2015) tested a closed-loop proportional integral derivative input shaper against external disturbances experimentally.

Böck and Kugi (2014) based the controller on a model that contains explicit differential equations. Its complexity is much lower than that of a full nonlinear model. The path-following controller is combined with the model predictive control and applied into a laboratory tower crane for evaluation. Bariša et al. (2014) decoupled the model into three subsystems, and the cross couplings between the equations were considered as a change in the system's parameters for each subsystem. The proposed nonlinear model predictive control was designed for each one and validated experimentally for the trolley subsystem. Breuning (2015) linearized the model to apply linear quadratic predictive control. Wu et al. (2016) used a linearized model for the construction of H∞-based adaptive fuzzy control technique which considers uncertainties, time delays, and external disturbances.

The preceding articles commonly developed their controllers based on simplified models, to simplify the control system design. The simplified models ignore nonlinear coupling dynamics by assuming small swing angle changes and the rate of change of the trolley position, and the jib rotation is of the same order of magnitude of the swing angles and their rates. The performance of the controllers based on these simplified or linearized models is degraded in the presence of uncertainties. The desired performance including the elimination of steady-state error and damping the oscillations can be achieved using high control effort. However, when the control demand is high, it will exceed the motors' capability and the desired performance will not be achieved. Therefore, the current work and the following literature focused on deriving various controllers based on the full nonlinear model without any simplification or linearization.

Le et al. (2013) designed two nonlinear controllers, partial feedback linearization and SMC, based on the full nonlinear model of the tower crane. However, the control effort for these controllers was not discussed, and the controllers were not applied experimentally. Also, the issue of steady-state error was not explicitly addressed that arise in real-life application. The SMC was presented by Utkin et al. (2009) that robustness can be achieved against uncertainties using a discontinuous control technique for several practical systems. Also, it constrains the system motion along the manifolds of reduced dimensionality in the state space.

Sun et al. (2016) has developed an adaptive control against parametric uncertainties using the full nonlinear model without simplifications. Le and Lee (2017) proposed a model reference adaptive-SMC for 4-DOF system, without experimental validation. Adaptive backstepping SMC is proposed for 2-DOF system by Bai and Ren (2018) to adapt the uncertainty due to the environmental interference with the tower crane operation and was tested experimentally.

The limitation of the SMC is being sensitive to noise and uncertainties during the reaching phase because the sliding mode is not realized. Eventually, when the uncertainties are large, the switching gain of SMC needs to be high for robustness. To make the SMC practically realizable, the switching gain should be limited, which results in degrading the performances of crane control. Therefore, integral sliding mode control (ISMC) was proposed by Utkin and Shi (1996), where the system trajectory always starts from the sliding surface and the reaching phase is eliminated.

Xi and Hesketh (2010) proposed ISMC for controlling overhead cranes which were developed for the single input single output system and any cross-coupling between the two motions in the multi input multi output model simply adds to the uncertainties. Integral sliding surface designs were developed for systems with matched and unmatched uncertainties, which might arise for imperfect modeling and external disturbances. Also, Sun et al. (2019) have introduced an integral term into the controller to overcome the steady state error that exists because of uncertainties.

This study presents the development of a robust control scheme for a four-DOF under-actuated tower crane system. The nonlinear controller is based on the high fidelity model without simplifications or linearization. The dynamic model of the system is derived using the Euler–Lagrange formulation with the consideration of friction. The ISMC is proposed to overcome the issue of steady-state error that arises in practical applications. The main aim of the controller is fast and accurate positioning of the payload to the desired final position while damping the oscillations, regardless of uncertainties. The stability of the closed-loop system is provided, including the designed controller and the integral terms. Also, Lyapunov-based stability analysis is used for coupled nonlinear under-actuated dynamics. The robustness of the controller is tested against uncertainties. Finally, a comparative assessment of the proposed controller with the conventional SMC is presented and validated experimentally.

This article is organized as follows: Section 2 introduces the tower crane system and the corresponding nonlinear dynamic model. The controller design process with stability analysis is presented in Section 3. In Section 4, the proposed control is evaluated through simulation and experimental results. Conclusions are drawn in Section 5.

2. Model

Dynamical equations are derived based on the Euler–Lagrange equation from Spong et al. (2006), resulting in four second-order nonlinear differential equations corresponding to four DOF

$$\frac{d}{dt}\left(\frac{\partial L}{\partial \dot{\vec{q}}}\right) - \frac{\partial L}{\partial \vec{q}} = \vec{u} - \left(B_{\vec{q}}\dot{\vec{q}} + \mu_{\vec{q}}\,\mathrm{sgn}\left(\dot{\vec{q}}\right)\right) \quad (1)$$

where $\vec{q}$ represents the joint angle vector including the four DOFs shown in Figure 1 $\vec{q} = [q_1 \quad q_2 \quad q_3 \quad q_4]^T = [x \quad \theta \quad \alpha \quad \beta]^T$. x is the position of the trolley, θ is the rotation of the jib around the z-axis, α is the in-plane oscillation, and β is the out-of-plane oscillation. $B_{\vec{q}}\dot{\vec{q}}$ represents the viscous friction and $\mu_{\vec{q}}\,\mathrm{sgn}(\dot{\vec{q}})$ represents the Coulomb friction. The input vector $\vec{u} = [u_1 \quad u_2 \quad 0 \quad 0]^T$ has only two control inputs which are the trolley driving force (u_1) and the tower rotating torque (u_2) respectively.

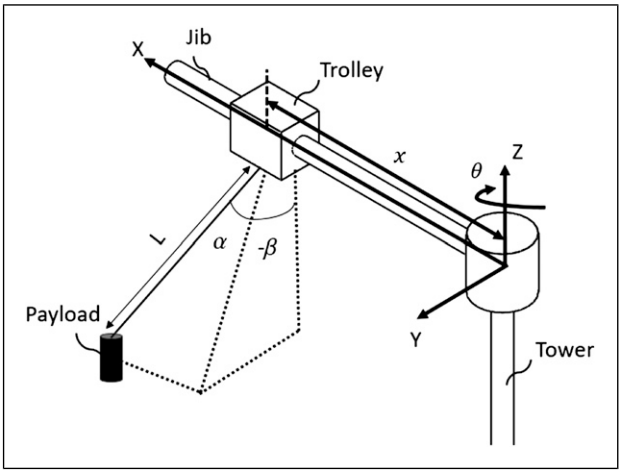

Figure 1. Degrees of freedom of tower crane.

Actuator dynamics are incorporated into the crane model and presented using equations (2) and (3).

$$u_1 = \frac{\eta_x K_{gx} K_{mx}}{R_{ax} r_x} G_{ax} U_x - \frac{\eta_x k_{gx}^2 k_{mx}^2}{R_{ax} r_x^2}\dot{x} \quad (2)$$

$$u_2 = \frac{\eta_\theta K_{g\theta} K_{m\theta}}{R_{a\theta}} G_{a\theta} U_\theta - \frac{\eta_\theta k_{g\theta}^2 k_{m\theta}^2}{R_{a\theta}}\dot{\theta} \quad (3)$$

where U_x is x-direction pulse width modulation (PWM) signal and U_θ is θ-direction PWM signal and the rest of the motor parameters with their values are presented in Table 1 and based on Breuning (2015). The dynamic model is represented in the form of

$$M(q)\ddot{q} + B(q,\dot{q}) + G(q) = u \quad (4)$$

where $M(q) \in R^{n\times n}$ is the inertia matrix which is a positive definite matrix for $L > 0$ and its inverse exists, $B(q,\dot{q}) \in R^{n\times 1}$ is the Coriolis, centripetal, and friction matrix, and $G(q) \in R^{n\times 1}$ is the gravitational force vector.

The DOFs consists of two vectors, actuated states (q_a) and unactuated states (q_u). The actuated states are the trolley position and the jib rotation, whereas the unactuated states are the swing angles of the payload

$$q_a = [x \quad \theta]^T, \quad q_u = [\alpha \quad \beta]^T \quad (5)$$

Therefore, equation (4) is arranged into two equations

$$M_{11}(q)\ddot{q}_a + M_{12}(q)\ddot{q}_u + B_{11}(q,\dot{q}) = u_a \quad (6)$$

$$M_{21}(q)\ddot{q}_a + M_{22}(q)\ddot{q}_u + B_{21}(q,\dot{q}) + G_2(q) = 0 \quad (7)$$

where

$$M_{11} = \begin{bmatrix} m_{11} & m_{12} \\ m_{21} & m_{22} \end{bmatrix}, \quad M_{12} = \begin{bmatrix} m_{13} & m_{14} \\ m_{23} & m_{24} \end{bmatrix},$$
$$M_{21} = \begin{bmatrix} m_{31} & m_{32} \\ m_{41} & m_{42} \end{bmatrix}, \quad M_{22} = \begin{bmatrix} m_{33} & m_{34} \\ m_{43} & m_{44} \end{bmatrix},$$
$$B_{11} = \begin{bmatrix} b_{11} \\ b_{21} \end{bmatrix}, \quad B_{21} = \begin{bmatrix} b_{31} \\ b_{41} \end{bmatrix},$$
$$u_a = \begin{bmatrix} F_x \\ F_\theta \end{bmatrix}, \quad G_2 = \begin{bmatrix} g_1 \\ g_2 \end{bmatrix}$$

The elements of the previous matrices and vectors are presented in Appendix 1. The control inputs have a direct effect on the actuated dynamics equation (6) whereas there

Table 1. Motor parameters.

Description	Value in x-direction	Value in θ-direction
Gear ratio	K_{gx} = 76.84	$K_{g\theta}$ = 275
Motor gearbox and motor efficiency	η_x = 0.36	η_θ = 0.24
Torque constant (Nm/A)	k_{mx} = 0.032	$k_{m\theta}$ = 0.0195
Radius of pulley	r_x = 0.0375 m	—
Armature resistance	R_{ax} = 25 Ω	$R_{a\theta}$ = 0.5 Ω
Amplifier gain	G_{ax} = 15	$G_{a\theta}$ = 12

is no effect on the unactuated dynamics equation (7). The following reformulation of the equations will allow the control inputs to affect the unactuated dynamics. Equations (6) and (7) are rewritten as follows

$$\ddot{q}_a = M_{11}^{-1}(q)(-M_{12}(q)\ddot{q}_u - B_{11}(q,\dot{q}) + u_a) \tag{8}$$

$$\ddot{q}_u = M_{22}^{-1}(q)(-M_{21}(q)\ddot{q}_a - B_{21}(q,\dot{q}) - G_2(q)) \tag{9}$$

Equation (9) is substituted into (6) and (8) is substituted into (7). The resulting equations are rearranged so that the system can be expressed as follows

$$\overline{M}_1(q)\ddot{q}_a + \overline{B}_{11}(q,\dot{q}) + G_1(q) = u_a \tag{10}$$

$$\overline{M}_2(q)\ddot{q}_u + \overline{B}_{21}(q,\dot{q}) + G_2(q) = u_u \tag{11}$$

where

$$\begin{aligned}
\overline{M}_1(q) &= M_{11}(q) - M_{12}(q)M_{22}(q)^{-1}M_{21}(q)\\
\overline{M}_2(q) &= M_{22}(q) - M_{21}(q)M_{11}(q)^{-1}M_{12}(q)\\
\overline{B}_{11}(q,\dot{q}) &= -M_{12}(q)M_{22}(q)^{-1}B_{21}(q,\dot{q}) + B_{11}(q,\dot{q})\\
\overline{B}_{21}(q) &= -M_{21}(q)M_{11}(q)^{-1}B_{11}(q,\dot{q}) + B_{21}(q,\dot{q})\\
G_1 &= -M_{12}(q)M_{22}(q)^{-1}G_2(q)\\
u_u &= -M_{21}(q)M_{11}(q)^{-1}u_a
\end{aligned}$$

The unactuated dynamics in equation (11) are indirectly affected by the control inputs.

3. Control system design

The antisway controllers are designed based on the nonlinear dynamical model in equations (10) and (11), without any simplification or linearization. The designed controllers are the SMC and ISMC. The stability is demonstrated using Lyapunov's method.

3.1. Conventional sliding mode control

The main aim of the controller is reaching the desired position of the actuated states while eliminating the unactuated states, increasing the complexity of the control design. The error vectors are defined as follows

$$e_a = q_a - q_{ad} = [x - x_d \quad \theta - \theta_d]^T \tag{12}$$

$$e_u = q_u - q_{ud} = [\alpha \quad \beta]^T \tag{13}$$

which e_a is the tracking error of the actuated states. The desired positions of the trolley and jib are x_d and θ_d respectively. e_u is the error of the unactuated states where the desired swing angles are equal to zero. The sliding surface is defined to be

$$s = \dot{e}_a + \lambda_1 e_a + \alpha\dot{e}_u + \lambda_2 e_u \tag{14}$$

where $\lambda_1, \lambda_2 \in R^+$ are the positive control parameters affecting the rate in which the states reach the desired position and α is the positive control parameter affecting the rate in which the states will settle, which are described by $\lambda_1 = \mathrm{diag}(\lambda_{11}, \lambda_{12})$, $\lambda_2 = \mathrm{diag}(\lambda_{21}, \lambda_{22})$, and $\alpha = \mathrm{diag}(\alpha_1, \alpha_2)$.

The problem of conventional SMC is the error will not coincide with the switching surface in the presence of uncertainties. Hence, steady-state error appears in the system's output. Therefore, the integral sliding mode is proposed to preserve the performance despite the uncertainties.

3.2. Integral sliding mode control

The dynamical model is updated as follows

$$M(q)\ddot{q} + B(q,\dot{q}) + G(q) + h(q,\dot{q},\ddot{q}) = u \tag{15}$$

to include the uncertainties term, $h \in R^{n\times 1}$. The actual value of $h(q,\dot{q},\ddot{q})$ is unknown, but it is assumed that it is bounded by a known function $\|h(q,\dot{q},\ddot{q})\| \le \overline{h}(q,\dot{q},\ddot{q})$. Utkin and Shi (1996) defined the switching function as follows

$$s = \dot{e} + K_p e + K_i \int_0^t e(\zeta)d\zeta \tag{16}$$

where K_p, $K_i \in R^+$ are the proportional and the integral control gains respectively. The system is third-order relative to the variable of interest $\int_0^t e dt$ as explained by Slotine et al. (1991).

The design of the controller is based on Lyapunov's method by considering

$$V = \frac{1}{2}s^T s \tag{17}$$

as a positive definite Lyapunov function, and $V(x)$ is radially unbounded. The sliding manifold for the tower crane system is defined as follows

$$s = \dot{e}_a + \lambda_1 e_a + \lambda_2 \int_0^t e_a dt + \alpha\dot{e}_u + \lambda_3 e_u \tag{18}$$

The Lyapunov function differentiated with respect to time is given as

$$\dot{V} = s\dot{s} \tag{19}$$

The time derivative of the sliding surface is obtained as

$$\dot{s} = \ddot{q}_a + \lambda_1\dot{q}_a + \lambda_2(q_a - q_{ad}) + \alpha\ddot{q}_u + \lambda_3\dot{q}_u \tag{20}$$

where the first and second derivatives of the desired values are set to zero. The equations of motion of system (10) and (11) are substituted into the equation of $\dot{s}$. Also, $\dot{s}$ should be in terms of the actuated control input u_a only. Hence, u_u is substituted by $-M_{21}(q)M_{11}(q)^{-1}u_a$. The resulting equation for $\dot{s}$ is substituted in $\dot{V}$

$$\begin{aligned}
\dot{V} = s\big[&u_a\big[\overline{M}_1(q)^{-1} - \alpha\overline{M}_2(q)^{-1}M_{21}(q)M_{11}(q)^{-1}\big]\\
&+ \overline{M}_1(q)^{-1}\big[-\overline{B}_{11}(q,\dot{q}) - G_1(q)\big] + \lambda_1\dot{q}_a + \lambda_3\dot{q}_u\\
&+ \alpha\big[\overline{M}_2(q)^{-1}\big[-\overline{B}_{21}(q,\dot{q}) - G_2(q)\big]\big]\\
&+ \lambda_2(q_a - q_{ad})\big]
\end{aligned} \tag{21}$$

In the sliding phase, the time derivative of s on the system trajectories should be made equal to zero to force the states to remain at the desired position. The error dynamics is

$$\ddot{e} + K_v\dot{e} + K_p e = 0 \tag{22}$$

The controller gains K_p and K_v are chosen properly for the characteristic equation (22) is strictly stable. The roots of the characteristic equation are in the left half plane (LHP) which implies that $\lim_{t\to\infty} e(t) = 0$.

The controller is designed as $u_a = \overrightarrow{u} + u_s$ where the nominal control $\overrightarrow{u}$ is defined using the computed torque method and responsible for the performance of the nominal system. The algebraic equation (21) is set to zero and solved with respect to the control input, the resulting control law is presented in equation (23). The nominal control law is designed for all $|\alpha| < \pi/2$ and $|\beta| < \pi/2$. u_s is equal to $-K\,\mathrm{sgn}(s)$ which is the discontinuous part to ensure that the states remain on the sliding surface

$$\begin{aligned} u_a = {} & \left(\overline{M}_1(q)^{-1} - \alpha\overline{M}_2(q)^{-1}M_{21}(q)M_{11}(q)^{-1}\right)^{-1} \\ & \left[\overline{M}_1(q)^{-1}\left[\overline{B}_{11}(q,\dot{q}) + G_1(q)\right] - \lambda_1\dot{q}_a - \lambda_3\dot{q}_u\right. \\ & \left. + \alpha\left[\overline{M}_2(q)^{-1}\left[\overline{B}_{21}(q,\dot{q}) + G_2(q)\right]\right]\right. \\ & \left. - \lambda_2(q_a - q_{ad})\right] - K\,\mathrm{sgn}(s) \end{aligned} \tag{23}$$

where $K = \mathrm{diag}(K_1, K_2) \in R^{n\times n}$ is a positive definite diagonal matrix with its diagonal elements satisfying $K_i > |h(q,\dot{q},\ddot{q})|$.

Controller equation (23) is substituted into the derivative of Lyapunov function (21)

$$\begin{aligned} \dot{V} &= s[-K\,\mathrm{sgn}(s) + F] \\ &\le (F - K)|s| < 0 \\ &\le -\mu_0|s| < 0 \end{aligned} \tag{24}$$

Some terms will not be canceled because of modeling uncertainties, the upper bound is denoted by F. If gain K is designed to be $K = F + \mu_0$, where $\mu_0 > 0$ and chosen to be a diagonal positive definite matrix, then the derivative of the Lyapunov function is ensured to remain negative definite. The time derivative $\dot{V} = s^T\dot{s} < 0$ is negative definite. Based on the definition from Khalil (2002), the closed loop system is guaranteed to be globally asymptotically stable. The controller in equation (25) guarantees that the stability of the system trajectories by proper selection of α so that the inverse of the matrix $\overline{M}_1(q)^{-1} - \alpha\overline{M}_2(q)^{-1}M_{21}(q)M_{11}(q)^{-1}$ exists.

The main drawback of the high frequency switching control actions in the integral sliding mode is the chattering phenomena due to unmodeled dynamics. The sign function is replaced by a saturation function to avoid chattering in the control input

$$\begin{aligned} u_a = {} & \left(\overline{M}_1(q)^{-1} - \alpha\overline{M}_2(q)^{-1}M_{21}(q)M_{11}(q)^{-1}\right)^{-1} \\ & \left[\overline{M}_1(q)^{-1}\left[\overline{B}_{11}(q,\dot{q}) + G_1(q)\right] - \lambda_1\dot{q}_a - \lambda_2(q_a - q_{ad})\right. \\ & \left. + \alpha\left[\overline{M}_2(q)^{-1}\left[\overline{B}_{21}(q,\dot{q}) + G_2(q)\right]\right]\right. \\ & \left. - \lambda_3\dot{q}_u\right] - K\,\mathrm{sat}(s,\epsilon) \end{aligned} \tag{25}$$

where

$$\mathrm{sat}(s,\epsilon) = \begin{cases} s/\epsilon, & \text{for } |s/\epsilon| \le 1 \\ \mathrm{sgn}(s/\epsilon), & \text{for } |s/\epsilon| > 1 \end{cases} \tag{26}$$

The proposed control guarantees that the tracking errors converge into a boundary layer whose thickness can be arbitrarily set by a positive constant ϵ.

3.3. Stability analysis

From the control law design, it can be concluded that the closed-loop system is globally asymptotically stable. Moreover, Almutairi and Zribi (2009) explains that the under-actuated system's states that are on the sliding surface converge to their desired values by satisfying the sufficient conditions on the control gains. The sufficient conditions is derived by combining the sliding surface equation (18) with two unactuated acceleration vector equation (7). Hence, the trajectories on the sliding surface are considered, and equation (18) is set to zero ($s = 0$) and $\dot{q}_{ad} = 0$

$$\begin{aligned} \dot{q}_a = {} & -\lambda_1(q_a - q_{ad}) - \lambda_2\int_0^t (q_a - q_{ad})dt \\ & - \alpha\dot{q}_u - \lambda_3 q_u \end{aligned} \tag{27}$$

From equations (9), (10), and (25), the unactuated acceleration equation can be written as

$$\begin{aligned} \ddot{q}_u &= M_{22}^{-1}(q)(-M_{21}(q)\ddot{q}_a - B_{21}(q,\dot{q}) - G_2(q)) \\ &= M_{22}^{-1}(q)(-M_{21}(q)[\overline{M}_1(q)^{-1}\left(u_a - \overline{B}_{11}(q,\dot{q})\right. \\ &\quad \left. - G_1(q)\right)] - B_{21}(q,\dot{q}) - G_2(q)) \\ &= M_{22}^{-1}(q)(-M_{21}(q)[\overline{M}_1(q)^{-1}((\overline{M}_1(q)^{-1} \\ &\quad - \alpha\overline{M}_2(q)^{-1}M_{21}(q)M_{11}(q)^{-1})^{-1}[\overline{M}_1(q)^{-1}[\overline{B}_{11}(q,\dot{q}) \\ &\quad + G_1(q)] - \lambda_1\dot{q}_a - \lambda_2(q_a - q_{ad}) + \alpha[\overline{M}_2(q)^{-1}[\overline{B}_{21}(q,\dot{q}) \\ &\quad + G_2(q)]] - \lambda_3\dot{q}_u] - \overline{B}_{11}(q,\dot{q}) - G_1(q))] \\ &\quad - B_{21}(q,\dot{q}) - G_2(q)) = h_1(x) \end{aligned} \tag{28}$$

Let

$$x = \begin{bmatrix} x_1 \\ x_2 \\ x_3 \\ x_4 \end{bmatrix} = \begin{bmatrix} q_u \\ \dot{q}_u \\ \int_0^t (q_a - q_{ad}) \\ q_a - q_{ad} \end{bmatrix} \tag{29}$$

Equation (28) is rewritten in terms of x only. Also, equation (27) is rewritten as

$$\dot{x}_4 = -\lambda_1 x_4 - \lambda_2 x_3 - \alpha x_2 - \lambda_3 x_1 = h_2(x) \tag{30}$$

Equations (28)–(30) are combined to get an autonomous system

$$\dot{x} = \begin{bmatrix} x_2 \\ h_1(x) \\ x_4 \\ h_2(x) \end{bmatrix} = f(x) \tag{31}$$

Linearize the system (31) about the equilibrium point to get $\dot{x} = Ax$, where

$$A = \left.\frac{\partial f(x)}{\partial x}\right|_{x=0} = \begin{bmatrix} 0_{2\times2} & I_{2\times2} & 0_{2\times2} & 0_{2\times2} \\ A_1 & A_2 & A_3 & A_4 \\ 0_{2\times2} & 0_{2\times2} & 0_{2\times2} & I_{2\times2} \\ -\lambda_3 & -\alpha & -\lambda_2 & -\lambda_1 \end{bmatrix} \tag{32}$$

where

$$\begin{aligned} A_1 &= \frac{\partial h_1(x)}{\partial x_1} = \begin{bmatrix} a_{11} & 0 \\ 0 & a_{12} \end{bmatrix} \\ A_2 &= \frac{\partial h_1(x)}{\partial x_2} = \begin{bmatrix} a_{21} & 0 \\ 0 & a_{22} \end{bmatrix} \\ A_3 &= \frac{\partial h_1(x)}{\partial x_3} = \begin{bmatrix} a_{31} & 0 \\ 0 & a_{32} \end{bmatrix} \\ A_4 &= \frac{\partial h_1(x)}{\partial x_4} = \begin{bmatrix} a_{41} & 0 \\ 0 & a_{42} \end{bmatrix} \end{aligned} \tag{33}$$

where

$$\begin{aligned} a_{11} &= \frac{-(Lm_2(g+\lambda_{11}\lambda_{31}))}{(m_2L(L-\alpha_1)+J_2)} \\ a_{12} &= \frac{-(Lm_2(g+x_d\lambda_{12}\lambda_{32}))}{(J_2+L^2m_2-Lx_d\alpha_2m_2)} \\ a_{21} &= \frac{-(B_a-L\lambda_{31}m_2+L\alpha_1\lambda_{11}m_2)}{(m_2L^2-\alpha_1m_2L+J_2)} \\ a_{22} &= \frac{-(B_b-Lx_d\lambda_{32}m_2+Lx_d\alpha_2\lambda_{12}m_2)}{(J_2+L^2m_2-Lx_d\alpha_2m_2)} \\ a_{31} &= \frac{-(L\lambda_{11}\lambda_{21}m_2)}{(m_2L^2-\alpha_1m_2L+J_2)} \\ a_{32} &= \frac{-(L\lambda_{12}\lambda_{22}m_2x_d)}{(J_2+L^2m_2-Lx_d\alpha_2m_2)} \\ a_{41} &= \frac{\left(Lm_2\left(-\lambda_{11}^2+\lambda_{21}\right)\right)}{(m_2L^2-\alpha_1m_2L+J_2)} \\ a_{42} &= \frac{\left(Lm_2x_d\left(-\lambda_{12}^2+\lambda_{22}\right)\right)}{(J_2+L^2m_2-Lx_d\alpha_2m_2)} \end{aligned} \tag{34}$$

The stability of the linearized system $\dot{x} = Ax$ is guaranteed when the linearized state matrix A should have its eigenvalues in the LHP of the complex plane. Using the Routh–Hurwitz criterion, the characteristic equation of the linearized system is calculated by $\det(sI - A) = 0$. The analysis gives sufficient conditions shown in equation (35). The parameters α, λ_1, λ_2, and λ_3 are chosen to satisfy the following conditions

$$\begin{aligned} &L^2\lambda_{11}m_2 + B_a + \lambda_{11}J_2 > \lambda_{31}Lm_2 \\ &L^2\lambda_{12}m_2 + B_b + \lambda_{12}J_2 > \lambda_{32}Lm_2x_d \\ &L^2m_2 + J_2 > \alpha_1Lm_2 \\ &L^2m_2 + J_2 > \alpha_2Lm_2x_d \end{aligned} \tag{35}$$

Because the linearized system is proven to be asymptotically stable, x converges to zero asymptotically. Therefore, from equation (29), q_a converges to q_{ad} and q_u, $\dot{q}_u$ converges to zero as t goes to infinity. From equation (27), $\dot{q}_a$ converges to zero as t goes to infinity. Hence, the integral sliding mode controller in equation (25) guarantees the asymptotic stability of the tower crane system. The sufficient conditions imposed by equation (35) guarantee that q_a, $\dot{q}_a$, q_u, and $\dot{q}_u$ reach their desired values as t goes to infinity.

4. Results and discussion

The controllers are implemented using MATLAB/simulink environment. The solver used is discrete: ode4 (Runge–Kutta algorithm) with a sampling time of 1 ms. The results presented are for the simultaneous motion where the trolley translation and the jib rotation are both excited at the same time. During all simulations and experiments, (1) the length is kept constant with a value of 0.5 m, (2) The desired position for the trolley is 0.3 m, (3) the desired position for the jib is 135°, and (5) the simulation time is 30 s.

The crane's parameters used in the model equations are given in Table 2. Altaf (2010) estimated the parameters using the prediction error method. Other parameters such as friction coefficients and the inertia are estimated using an offline identification parameter estimation tool in MATLAB via the sum square method based on the structure of the model.

4.1. Robustness of ISMC

During simulations, the uncertainties are represented by the friction model. In other words, the controllers are based on the model without the friction model. The controllers are tested at two different values of the boundary layers. When uncertainties are added to the system, the SMC results at the boundary layer equal to 2 show that the trolley position has a steady-state error of 0.02 m and the jib rotation has a steady-state error of 8°. Therefore, the boundary layer has been reduced to 0.5. As shown from Figures 2 and 3,

Table 2. Model parameters.

Description	Value
Mass of the trolley	m_1 = 0.7 kg
Mass of the payload	m_2 = 0.32 kg
Coulomb friction coefficient in x-direction	μ_x = 0.36 Nm/s
Coulomb friction coefficient in θ-direction	μ_θ = 0.9 Nm/s
Viscous friction coefficient in x-direction	B_x = 34 Nm/s
Viscous friction coefficient in θ-direction	B_θ = 18 Nm/s
Viscous friction coefficient in α-direction	B_α = 0.0015 Nm/s
Viscous friction coefficient in β-direction	B_β = 0.0015 Nm/s
Jib's moment of inertia	J_1 = 4 kgm^2
Load's moment of inertia	J_2 = 0.02 kgm^2
Gravitational constant	g = 9.81 m/s^2

the steady-state error has been successfully eliminated. However, Figures 4 and 5 show that with a smaller boundary layer, the control effort demand has been increased.

The results of ISMC shows that there is no steady-state error in the position of the trolley and the jib. Also, the control effort demand is low compared with the SMC. Therefore, ISMC shows better results than conventional SMC. These results include reducing the control effort demand from 16 N to 8.6 N for the trolley and 30 N to 17.6 N for the jib rotation. Also, It shows that the effects of the uncertainties are suppressed by the proposed ISMC. The rise time for the two controllers using different boundary layers are almost equal to 2.5 s, so they are capable of fast maneuvers. The alpha oscillations are damped after 18 s and the beta oscillations are damped after 6.8 s.

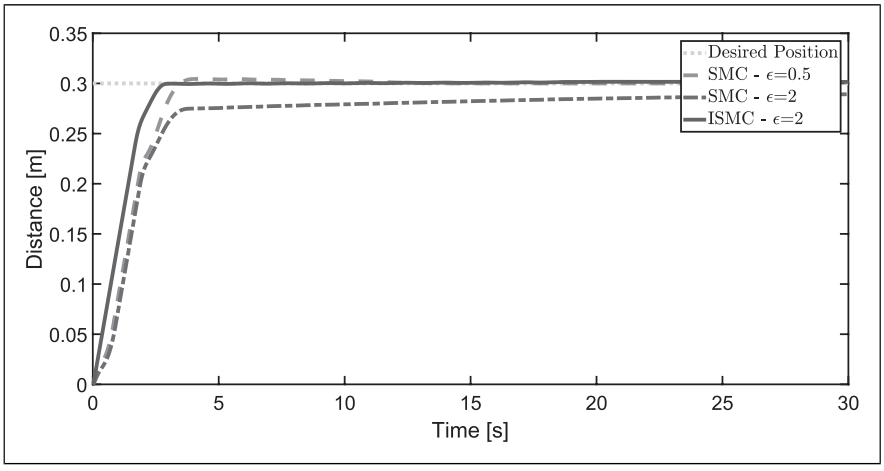

Figure 2. Trolley position including uncertainties in the model with a boundary layer thickness of 0.5 and 2.

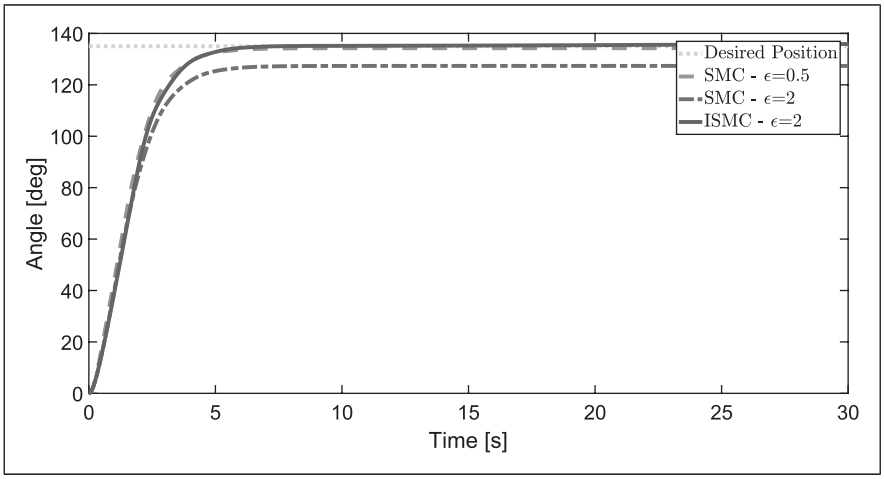

Figure 3. Jib rotation including uncertainties in the model with a boundary layer thickness of 0.5 and 2.

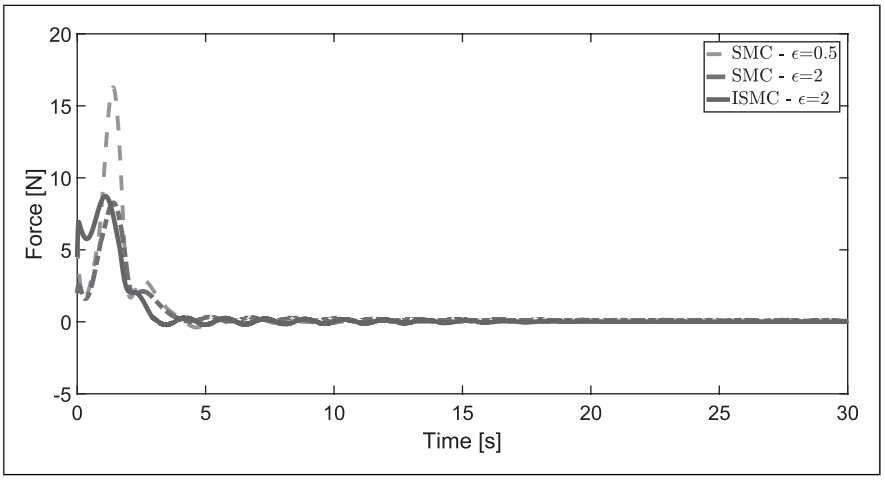

Figure 4. Control input required to move the trolley.

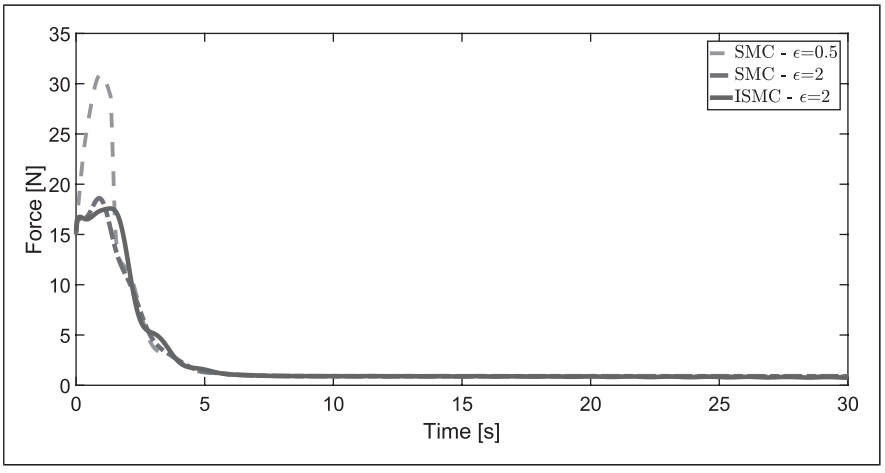

Figure 5. Control input required to rotate the jib.

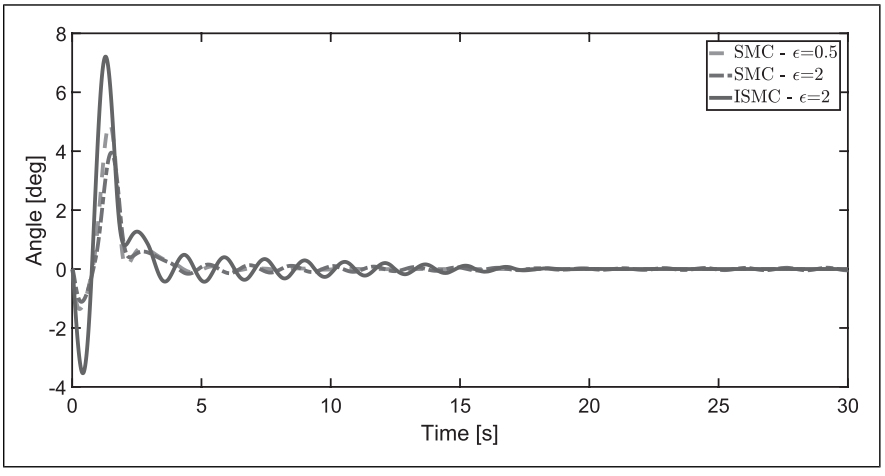

Figure 6. Alpha oscillations including uncertainties in the model with a boundary layer thickness of 0.5 and 2.

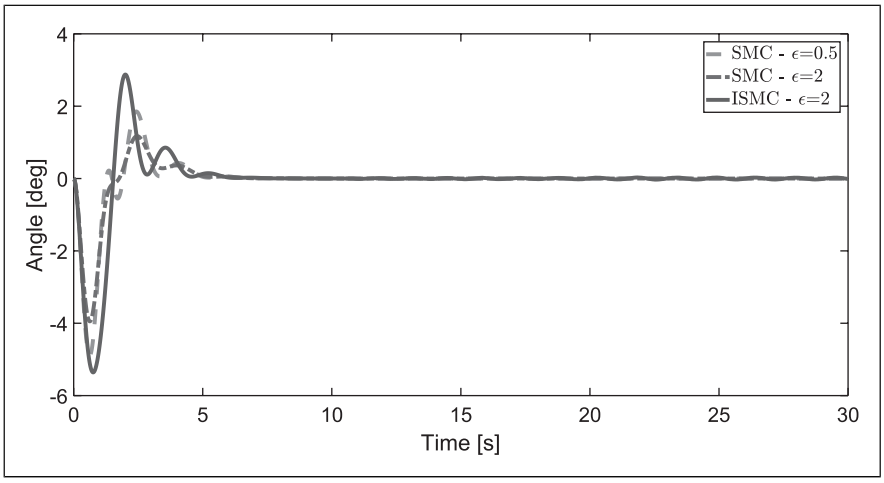

Figure 7. Beta oscillations including uncertainties in the model with a boundary layer thickness of 0.5 and 2.

Therefore, the controllers have successfully damped the oscillations of the payload at the destination as shown in Figures 6 and 7.

4.2. Experimental validation

The SMC and ISMC are implemented for the real setup. The unmodeled uncertainties are the difference between the real system and the derived full nonlinear model.

4.3. Hardware

The test bench is a laboratory INTECO tower crane shown in Figure 8. The feedback for the position of the states (x, θ, α, and β) are measured by high-resolution encoders. All the experiments are conducted in real time where the simulink model is converted into C code to get the required signals using a built-in C compiler toolbox in MATLAB. The interface board sends the output signals to the actuators, which control the crane's movement. Then the controllers' outputs are plotted against each other. The initial trolley position is set to 0.22 m whereas the initial jib position and the initial payload swings are set to zero.

The experimental results of the SMC results with the boundary layer are equal to 2, show that the trolley position has a steady-state error of 0.03 m and the jib rotation have an error of 2°. When the boundary layer is reduced to 0.5 as shown from Figures 9 and 10, the steady-state error is not eliminated for the trolley but successfully eliminated for the jib rotation. However, Figures 11 and 12 show that with a smaller boundary layer, the control effort demand has been increased. The results of ISMC shows that there is no steady-state error in the position of the trolley and the jib. In addition, the control effort demand is reduced from 7 to 4 N for the trolley input and from 20 to 10 N. There is no overshoot in any of the experiments. Also, the residual oscillations in the swing angles are very small ranging between almost −0.5 and 0.5°. As shown in Figures 13 and 14, they are hardly observed in reality.

Figure 8. Tower crane inteco setup.

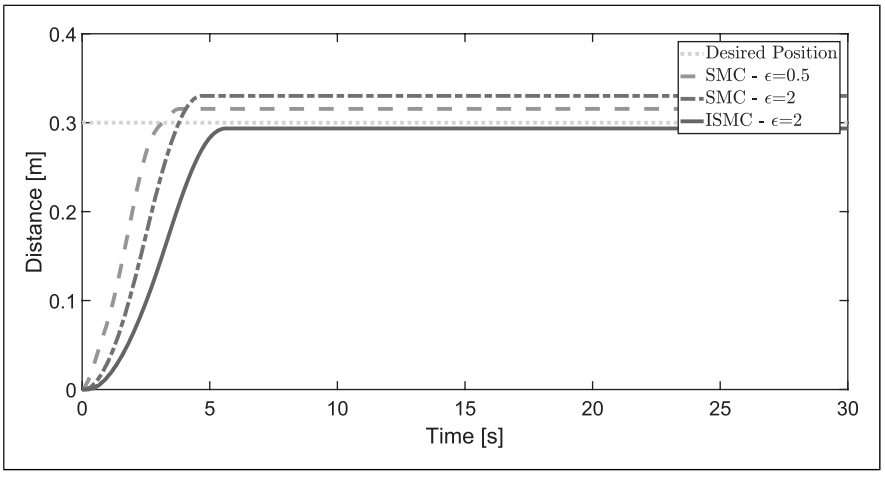

Figure 9. Experimental results of the trolley position with a boundary layer thickness of 0.5 and 2.

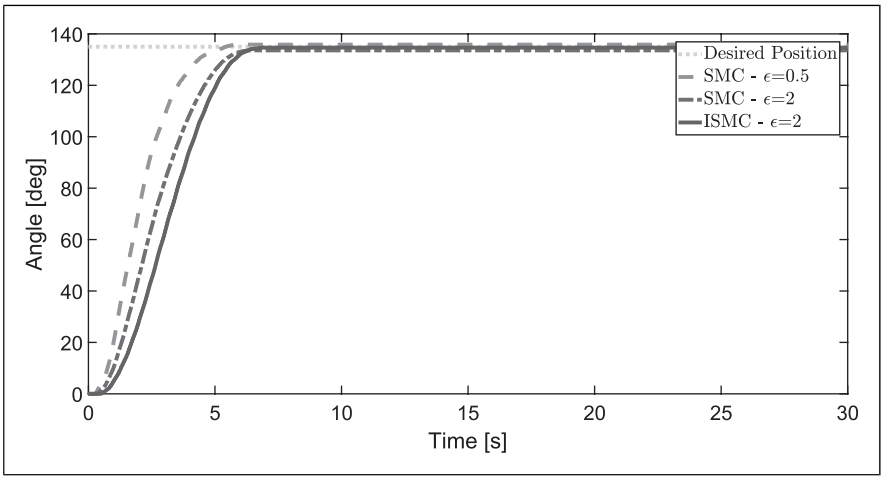

Figure 10. Experimental results of the jib position with a boundary layer thickness of 0.5 and 2.

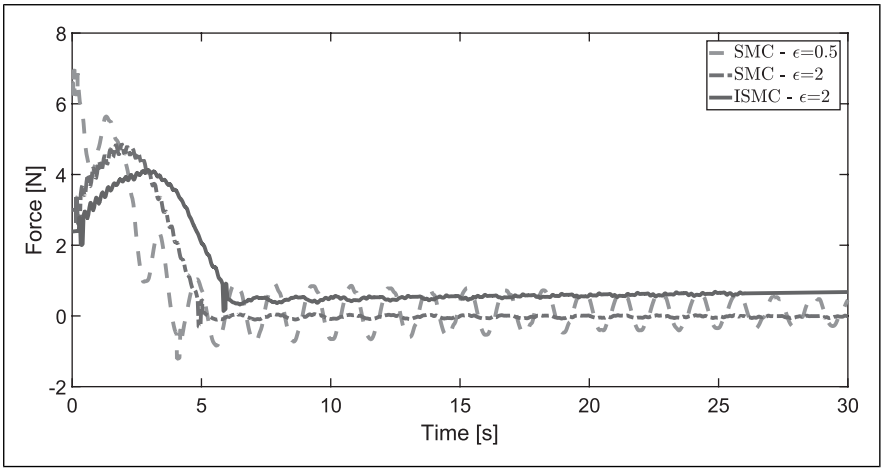

Figure 11. Experimental control input required to move the trolley.

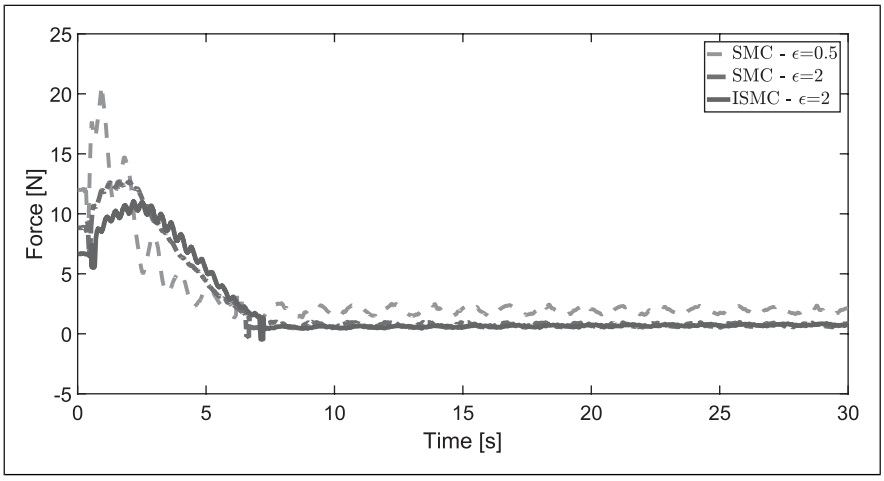

Figure 12. Experimental control input required to rotate the jib.

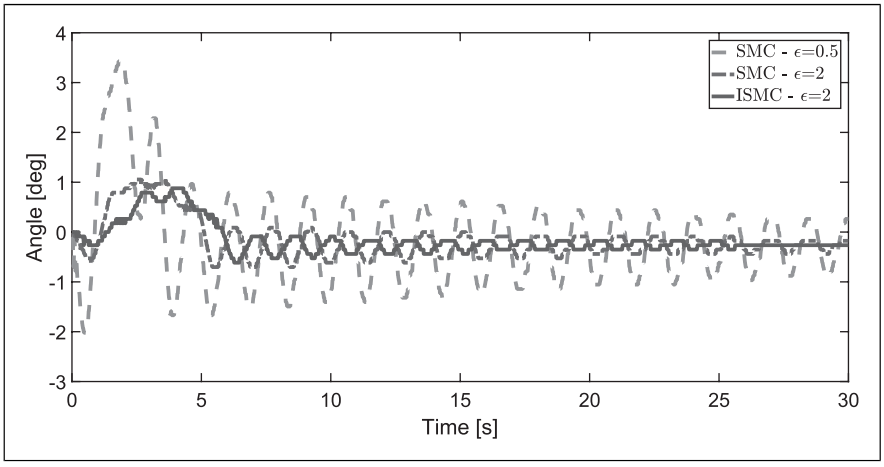

Figure 13. Experimental results of the alpha oscillations with a boundary layer thickness of 0.5 and 2.

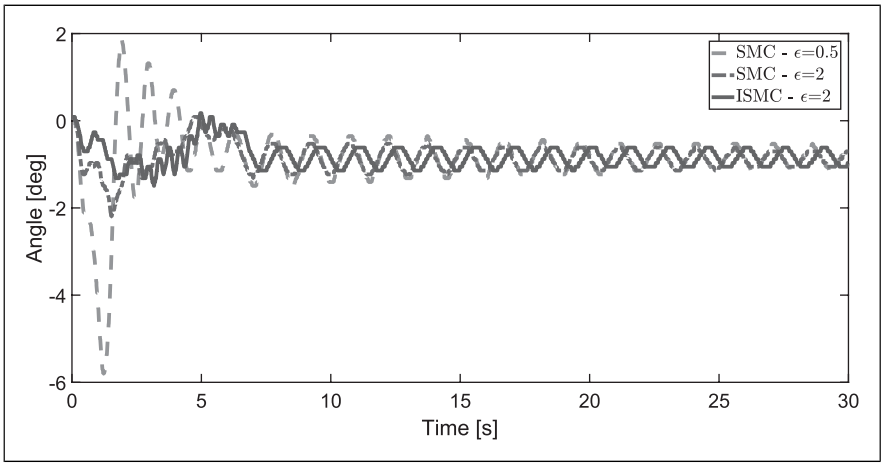

Figure 14. Experimental results of the beta oscillations with a boundary layer thickness of 0.5 and 2.

5. Conclusion

Nonlinear robust controllers are implemented for precise tracking of the desired position while damping the payload oscillations in fast maneuvers. These controllers are derived based on the nonlinear dynamical model without any linearization or decoupling to reduce the model uncertainties. The problem with a high value of model uncertainties is that the switching gain must be high for robustness. However, the switching gain must be limited to implement the SMC on the real system, resulting in the steady-state error existence in the system's outputs. Therefore, the ISMC is proposed which enhances the performance of the tower crane system against uncertainties. The simulation and experimental results of the ISMC show that the steady-state error was eliminated while maintaining a low control effort demand, compared with the conventional SMC.

Declaration of conflicting interests

The author(s) declared no potential conflicts of interest with respect to the research, authorship, and/or publication of this article.

Funding

The author(s) received no financial support for the research, authorship, and/or publication of this article.

ORCID iD

Ayman A El-Badawy https://orcid.org/0000-0001-7288-7841

References

Abdel-Rahman EM, Nayfeh AH and Masoud ZN (2003) Dynamics and control of cranes: a review. *Journal of Vibration and control* 9(7): 863–908.

Ahmad MA, Ramli MS, Ismail RMTR, et al. (2015) Trajectory control and sway suppression of a rotary crane system. In: *Machine Vision and Mechatronics in Practice*. Berlin, Heidelberg: Springer, 165–175.

Aksjonov A, Vodovozov V and Petlenkov E (2015) Three-dimensional crane modelling and control using Euler–Lagrange state-space approach and anti-swing fuzzy logic. *Electrical, Control and Communication Engineering* 9(1): 5–13.

Al-Mousa AA (2000) *Control of rotary cranes using fuzzy logic and time-delayed position feedback control*. PhD Thesis, Virginia Polytechnic Institute and State University, Blacksburg, Virginia.

Almutairi NB and Zribi M (2009) Sliding mode control of a three-dimensional overhead crane. *Journal of vibration and control* 15(11): 1679–1730.

Altaf F (2010) *Modeling and event-triggered control of multiple 3D tower cranes over WSNs*. Master's Thesis, School of Electrical Engineering, Stockholm, Sweden.

Antic D, Jovanovic Z, Peric S, et al. (2012) Anti-swing fuzzy controller applied in a 3D crane system. *Engineering, Technology & Applied Science Research* 2(2): 196–200.

Bai WW and Ren HP (2018) Horizontal positioning and anti-swinging control tower crane using adaptive sliding mode control. In: 2018 Chinese control and decision conference (CCDC), Shenyang, China, 9–11 June 2018, pp. 4013–4018. IEEE.

Bariša T, Bartulović M, Žužić G, et al. (2014) Nonlinear predictive control of a tower crane using reference shaping approach. In: 2014 16th international power electronics and motion control conference and exposition (PEMC), Antalya, Turkey, 21–24 September 2014, pp. 872–876. IEEE.

Böck M and Kugi A (2014) Real-time nonlinear model predictive path-following control of a laboratory tower crane. *IEEE Transactions on Control Systems Technology* 22(4): 1461–1473.

Breuning P (2015) *Linear model predictive control of a 3D tower crane for educational use*. PhD Thesis, University of Stuttgart, Stuttgart, Germany.

Cho HC and Lee KS (2008) Adaptive control and stability analysis of nonlinear crane systems with perturbation. *Journal of Mechanical Science and Technology* 22(6): 1091: 1098.

Elbadawy AA and Shehata MM (2015) Anti-sway control of marine cranes under the disturbance of a parallel manipulator. *Nonlinear Dynamics* 82(1–2): 415–434.

Golafshani AR and Aplevich J (1995) Computation of time-optimal trajectories for tower cranes. In: Proceedings of international conference on control applications, Albany, NY, USA, 28–29 September 1995, pp. 1134–1139. IEEE.

He W, Meng T, He X, et al. (2018) Unified iterative learning control for flexible structures with input constraints. *Automatica* 96: 326–336.

He W, Zhang S and Ge SS (2014) Robust adaptive control of a thruster assisted position mooring system. *Automatica* 50(7): 1843–1851.

Khalil HK (2002) *Nonlinear Systems*. 3rd edition. upper Saddle River, NJ: Prentice-Hall.

Le AT and Lee S-G (2017) 3d cooperative control of tower cranes using robust adaptive techniques. *Journal of the Franklin Institute* 354(18): 8333–8357.

Le AT, Moon SC, Kim DH, et al. (2012) Adaptive sliding mode control of three dimensional overhead cranes. In: 2012 IEEE international conference on cyber technology in automation, control, and intelligent systems (CYBER), Bangkok, Thailand, 27–31 May 2012, pp. 354–359. IEEE.

Le TA, Dang V-H, Ko DH, et al. (2013) Nonlinear controls of a rotating tower crane in conjunction with trolley motion. *Proceedings of the Institution of Mechanical Engineers, Part I: Journal of Systems and Control Engineering* 227(5): 451–460.

Omar HM and Nayfeh AH (2005) Anti-swing control of gantry and tower cranes using fuzzy and time-delayed feedback with friction compensation. *Shock and Vibration* 12(2): 73–89.

Parker GG, Petterson B, Dohrmann C, et al. (1995) Command shaping for residual vibration free crane maneuvers. In: Proceedings of the 1995 American control conference, Seattle, WA, USA, 21–23 June 1995, pp. 934–938. IEEE.

Qian D and Yi J (2016) *Hierarchical Sliding Mode Control for Under-actuated Cranes*. Heidelberg, Berlin: Springer.

Samin RE, Mohamed Z, Jalani J, et al. (2013) Input shaping techniques for anti-sway control of a 3-dof rotary crane system. In: 2013 1st international conference on artificial intelligence, modelling and simulation (AIMS), Kota Kinabalu, Malaysia, 3–5 December 2013, pp. 184–189. IEEE.

Slotine JJE and Li W (1991) *Applied Nonlinear Control*. Englewood Cliffs, NJ: Prentice-Hall.

Spong MW, Hutchinson S and Vidyasagar M (2006) *Robot Modeling and Control*. New York: Wiley, Vol. 3.

Sun N, Fang Y, Chen H, et al. (2016) Slew/translation positioning and swing suppression for 4-dof tower cranes with parametric uncertainties: Design and hardware experimentation. *IEEE Transactions on Industrial Electronics* 63(10): 6407–6418.

Sun N, Wu Y, Chen H, et al. (2019) Antiswing cargo transportation of under-actuated tower crane systems by a nonlinear controller embedded with an integral term. *IEEE transactions on automation science and engineering* 16(3): 1387–1398.

Utkin V, Guldner J and Shi J (2009) *Sliding Mode Control in Electro–Mechanical Systems*. Boca Raton, FL: CRC Press.

Utkin V and Shi J (1996) Integral sliding mode in systems operating under uncertainty conditions. In: Proceedings of 35th IEEE conference on decision and control, Kobe, Japan, 13–13 December 1996, pp. 4591–4596. IEEE.

Vaughan J, Kim D and Singhose W (2010) Control of tower cranes with double-pendulum payload dynamics. *IEEE Transactions on Control Systems Technology* 18(6): 1345–1358.

Vázquez C, Fridman L, Collado J, et al. (2015) Second-order sliding mode control of a perturbed-crane. *Journal of Dynamic Systems, Measurement, and Control* 137(8): 081010.

Wu T-S, Karkoub M, Yu W-S, et al. (2016) Anti-sway tracking control of tower cranes with delayed uncertainty using a robust adaptive fuzzy control. *Fuzzy Sets and Systems* 290: 118–137.

Xi Z and Hesketh T (2010) Discrete time integral sliding mode control for overhead crane with uncertainties. *IET Control Theory & Applications* 4(10): 2071–2081.

Yang JH and Yang KS (2007) Adaptive coupling control for overhead crane systems. *Mechatronics* 17(2): 143–152.

Appendix 1

Coefficients of $M(q)$ matrix are

$$
\begin{aligned}
m_{11} &= m_1 + m_2 \\
m_{12} &= m_{13} = m_{14} = m_{21} = 0 \\
m_{22} &= J_1 + \frac{3}{4}L^2 m_2 + m_1 x^2 + m_2 x^2 - \frac{1}{4}L^2 m_2 \cos(2\alpha) \\
&\quad - \frac{1}{2}L^2 m_2 \cos(\alpha)^2 \cos(2\beta) \\
m_{23} &= m_{32} = m_{34} = m_{41} = m_{43} = 0 \\
m_{24} &= L m_2 x \cos(\alpha)\cos(\beta) \\
m_{31} &= L m_2 \cos(\alpha) \\
m_{33} &= J_2 + L^2 m_2 \\
m_{42} &= L m_2 x \cos(\alpha)\cos(\beta) \\
m_{44} &= J_2 + L^2 m_2 \cos(\alpha)^2
\end{aligned}
$$

Coefficients of $B(q)$ matrix are

$$
\begin{aligned}
b_{11} &= B_x \dot{x} + \mu_x \operatorname{sgn}(\dot{x}) \\
b_{21} &= B_\theta \dot{\theta} + \mu_\theta \operatorname{sgn}\left(\dot{\theta}\right) + 2m_1 x\dot{x}\dot{\theta} + 2m_2 x\dot{x}\dot{\theta} \\
&\quad + 2L m_2 x \dot{\theta}\dot{\alpha}\cos(\alpha) \\
b_{31} &= B_\alpha \dot{\alpha} - L m_2 x \dot{\theta}^2 \cos(\alpha) \\
&\quad - 2L^2 m_2 \dot{\theta}\dot{\beta}\cos(\alpha)^2 \cos(\beta) \\
b_{41} &= 2L m_2 \dot{x}\dot{\theta}\cos(\alpha)\cos(\beta) \\
&\quad + 2L^2 m_2 \dot{\theta}\dot{\alpha}\cos(\alpha)^2 \cos(\beta) + B_\beta \dot{\beta}
\end{aligned}
$$

Coefficients of $G(q)$ are

$$
\begin{aligned}
g_1 &= g L m_2 \cos(\beta)\sin(\alpha) \\
g_2 &= g L m_2 \cos(\alpha)\sin(\beta)
\end{aligned}
$$